

Rothamsted Repository Download

A - Papers appearing in refereed journals

Button, E. S., Marsden, K. A., Nightingale, P. D., Dixon, E. R., Chadwick, D. R., Jones, D. L. and Cardenas, L. M. 2023. Separating N₂O production and consumption in intact agricultural soil cores at different moisture contents and depths. *European Journal of Soil Science*. 74 (2), p. e13363. <https://doi.org/10.1111/ejss.13363>

The publisher's version can be accessed at:

- <https://doi.org/10.1111/ejss.13363>


The output can be accessed at:

<https://repository.rothamsted.ac.uk/item/98w3q/separating-n2o-production-and-consumption-in-intact-agricultural-soil-cores-at-different-moisture-contents-and-depths>.

© 4 April 2023, Please contact library@rothamsted.ac.uk for copyright queries.

RESEARCH ARTICLE

Separating N₂O production and consumption in intact agricultural soil cores at different moisture contents and depths

Erik S. Button¹  | Karina A. Marsden¹ | Philip D. Nightingale² |
Elizabeth R. Dixon³ | David R. Chadwick¹ | David L. Jones^{1,4} |
Laura M. Cárdenas³

¹School of Natural Sciences, Bangor University, Bangor, Gwynedd, UK

²Plymouth Marine Laboratory, Prospect Pl, Marine Biogeochemical Observations, Plymouth, Devon, UK

³Rothamsted Research North Wyke, Net Zero and Resilient Farming, Okehampton, Devon, UK

⁴Centre for Sustainable Farming Systems, Food Futures Institute, Murdoch, Western Australia, Australia

Correspondence

Laura M. Cárdenas, Rothamsted Research North Wyke, Net Zero and Resilient Farming, Okehampton, Devon, EX20 2SB, UK.

Email: laura.cardenas@rothamsted.ac.uk

Funding information

Biotechnology and Biological Sciences Research Council; Welsh European Funding Office

Abstract

Agricultural soils are a major source of the potent greenhouse gas and ozone depleting substance, N₂O. To implement management practices that minimize microbial N₂O production and maximize its consumption (i.e., complete denitrification), we must understand the interplay between simultaneously occurring biological and physical processes, especially how this changes with soil depth. Meaningfully disentangling of these processes is challenging and typical N₂O flux measurement techniques provide little insight into subsurface mechanisms. In addition, denitrification studies are often conducted on sieved soil in altered O₂ environments which relate poorly to *in situ* field conditions. Here, we developed a novel incubation system with headspaces both above and below the soil cores and field-relevant O₂ concentrations to better represent *in situ* conditions. We incubated intact sandy clay loam textured agricultural topsoil (0–10 cm) and subsoil (50–60 cm) cores for 3–4 days at 50% and 70% water-filled pore space, respectively. ¹⁵N-N₂O pool dilution and an SF₆ tracer were injected below the cores to determine the relative diffusivity and the net N₂O emission and gross N₂O emission and consumption fluxes. The relationship between calculated fluxes from the below and above soil core headspaces confirmed that the system performed well. Relative diffusivity did not vary with depth, likely due to the preservation of preferential flow pathways in the intact cores. Gross N₂O emission and uptake also did not differ with depth but were higher in the drier cores, contrary to expectation. We speculate this was due to aerobic denitrification being the primary N₂O consuming process and simultaneously occurring denitrification and nitrification both producing N₂O in the drier cores. We provide further evidence of substantial N₂O consumption in drier soil but without net negative N₂O emissions. The results from this study are important for the future application of the ¹⁵N-

This is an open access article under the terms of the [Creative Commons Attribution](https://creativecommons.org/licenses/by/4.0/) License, which permits use, distribution and reproduction in any medium, provided the original work is properly cited.

© 2023 The Authors. *European Journal of Soil Science* published by John Wiley & Sons Ltd on behalf of British Society of Soil Science.

N₂O pool dilution method and N budgeting and modelling, as required for improving management to minimize N₂O losses.

KEYWORDS

denitrification, diffusion coefficient, isotope pool dilution, nitrogen cycling, sulphur hexafluoride

1 | INTRODUCTION

Nitrous oxide (N₂O) exchange between the soil and atmosphere has received significant attention in recent decades because of its prominent role in climate change and atmospheric ozone depletion (e.g., Jia et al., 2019). More than half of global agricultural greenhouse gas emissions are from N₂O, resulting from N inputs to soil, including fertilizer and manure application (direct) and denitrification following leaching and atmospheric deposition of nitrogen (N; indirect) (Clough et al., 2005; Jia et al., 2019). There are several pathways and processes (both biotic and abiotic) that produce and consume N₂O in soils (see Butterbach-Bahl et al., 2013), however, nitrification and denitrification are widely considered the major N₂O producing processes. Under suboxic conditions, the production of atmospheric N₂O is primarily governed by microbial incomplete denitrification in the soil, where N₂O is produced from nitrate (NO₃⁻) under partially anaerobic conditions (Table S1; Diba et al., 2011). Nitrification (Table S1) is an aerobic process, and some studies have shown it can be the dominant N₂O producing process (e.g., Liu et al., 2016; Zhang et al., 2016), especially where soil aeration is sufficient (35%–60% water-filled pore space [WFPS]; Bateman & Baggs, 2005). However, denitrifiers can also consume N₂O (i.e., complete denitrification; Table S1) to produce inert dinitrogen (N₂) gas (Diba et al., 2011), which constitutes 78% of the Earth's atmosphere. Typically, N₂ is the major end product of denitrification, where the soil moisture is greater than 80% WFPS (Giles et al., 2017) as it is performed by facultative anaerobic microorganisms (Butterbach-Bahl et al., 2013). This process is often masked by greater production rates and is mostly measured only when the consumption rate exceeds the production rate (i.e., net negative emissions; Chapuis-Lardy et al., 2007; Schlesinger, 2013). Measuring the consumption of N₂O directly (e.g., by N₂ flux) is challenging against a very high atmospheric background (Clough et al., 2006; Wen et al., 2016; Yang et al., 2011). In addition, the heterogeneity of N₂O processes in the soil and their measurement can lead to high error when data is scaled (Groffman et al., 2006). Accurately measuring N₂O consumption is important for modelling and prediction

Highlights

- Explores how N₂O diffusion, production and consumption vary with soil depth and soil moisture.
- A novel and more field-relevant system was developed to incubate intact top- and subsoil cores.
- Diffusion was driven by moisture and N₂O consumption and production were highest in drier soil.
- This new system can separate N₂O processes occurring at depth whilst replicating field conditions.

of future soil N budgets, for which N₂O is the most poorly constrained term, due to the abovementioned inherent challenges (Almaraz et al., 2020; Blagodatsky & Smith, 2012; Boyer et al., 2006).

The balance between gross production and consumption of N₂O in agricultural soil is complex, being influenced by a range of environmental factors (e.g., temperature, moisture, O₂ content; Chapuis-Lardy et al., 2007), soil characteristics (e.g., pH, mineral N content, porosity, organic matter content, soil depth; Chapuis-Lardy et al., 2007; Clough et al., 2005; Stuchiner & von Fischer, 2022a) and management practices (e.g., fertilizing regime, tillage, irrigation; Khalil et al., 2002; Wang et al., 2018).

The consumption of N₂O is stimulated by anaerobic conditions (high WFPS) due to the sensitivity of the metallo-enzyme, N₂O reductase, to O₂ (Richardson et al., 2009). Thus, extensively waterlogged soils, such as peat- and wetlands represent the greatest N₂O sinks globally (Schlesinger, 2013). Low mineral N content is also thought to be important for N₂O consumption, because nitrate (NO₃⁻) outcompetes N₂O as a terminal electron acceptor (Chapuis-Lardy et al., 2007). However, N₂O consumption has been found to coincide with low WFPS in both fertilized (<50% WFPS; Khalil et al., 2002) and unfertilised soil (5%–20% WFPS; Wu et al., 2013). Here,

anaerobic conditions may exist in microsites heterogeneously distributed throughout the soil profile of free-draining soils, within soil aggregates (even in dry aerobic soil; Sextstone et al., 1985) or can be caused by localized respiration hot spots that deplete O_2 (Clough et al., 1999; Hill & Cardaci, 2004; Van Cleemput, 1998). Therefore, N_2O produced in the soil is not necessarily consumed in the same location but may diffuse to another site in the soil, may be lost to the atmosphere or groundwater (Shcherbak & Robertson, 2019), or become entrapped in the soil (Clough et al., 1999). In addition, aerobic consumption of N_2O is possible, where N_2O is used as an electron acceptor when NO_3^- is limited (Chapuis-Lardy et al., 2007; Wang et al., 2018). To understand these processes in a meaningful way, the physical diffusion and the gross N_2O production and consumption rates need to be separated from each other.

N_2O processes occurring deeper in the soil have received less attention but are important in understanding the balance between N_2O production and consumption (Almaraz et al., 2020; Clough et al., 2005; Jahangir et al., 2012). The movement of N_2O to the soil surface is predominantly via passive diffusion through air-filled pores in the soil. The concentration of N_2O at depth is frequently higher than near the soil surface because of lower diffusivity (Balaine et al., 2013; Currie, 1984; Davidson et al., 2004; Dong et al., 2013; Fujikawa & Miyazaki, 2005; Laughlin & Stevens, 2002; van Bochove et al., 1998; Van Groenigen et al., 2005; Wang et al., 2018; Zona et al., 2013). This lag between production and surface emission is supported by a ^{15}N -labelled experiment by Clough et al. (1999), where it took 11 days for N_2O produced at 80 cm to first reach the soil surface and 6% remained in the soil even after 38 days (i.e., entrapment). Soil conditions restricting N_2O diffusion, thereby increasing its residence time in the soil, can increase its consumption (Chapuis-Lardy et al., 2007; Clough et al., 2005; Neftel et al., 2007). The generally higher rate of N_2O consumption and production in the topsoil is a reflection of the greater microbial abundance and activity (Van Beek et al., 2004; van Bochove et al., 1998; Wang et al., 2018) than in subsoils, but considerable N_2O production and consumption can also occur in the subsoil if conditions allow (Clough et al., 1999; Shcherbak & Robertson, 2019). In addition, an understanding of the relationship between diffusion and N_2O emissions is lacking (Balaine et al., 2013), especially in intact deep soil (Chamindu Deepagoda et al., 2019). Therefore, understanding the balance of N_2O production and consumption between topsoil and subsoil depths under different soil conditions and their relation to diffusion is needed to best predict N_2O surface emissions for modelling the global N budget (Almaraz et al., 2020; Blagodatsky & Smith, 2012; Boyer et al., 2006).

Understanding N_2O mechanisms in the soil is important for more accurate modelling and N budgeting, and to support emerging attempts to minimize N_2O losses from soil. Chamindu Deepagoda et al. (2019) found a range of relative gas diffusivity rates which lowered N_2O emissions that could be monitored and maintained by land users. Stuchiner and von Fischer (2022a) recently demonstrated a case of Increased Consumption and Decreased Emissions (coined ICDE) of N_2O via promotion of anoxia from relieving the C-limitation to the microbial community.

The $^{15}N_2O$ pool dilution method is a relatively new method used by Yang et al. (2011), Yang and Silver (2016), and Wen et al. (2016, 2017) to determine the gross production and consumption of N_2O . The method, where isotopically enriched $^{15}N_2O$ is injected into a closed system and the disappearance of the label is measured over time, is currently the only method for field measurement of gross N_2O emission and uptake under undisturbed conditions (Almaraz et al., 2020). This method can also be applied to the incubation of soil cores, as performed by Wen et al. (2016) and Stuchiner and von Fischer (2022a), which allows for the incubation of soil cores taken from below the surface. An inherent assumption of the $^{15}N_2O$ pool dilution method is that the $^{15}N_2O$ that diffuses into the soil mixes evenly with soil-derived N_2O . Wen et al. (2016) compared the pool dilution method with a gas-flow core method and found it to underestimate gross N_2O production and consumption. As a result of the use of a closed static system in previous applications of the method, the diffusion and mixing of the labelled gas with soil pores is less likely to occur, which means that gross N_2O production and consumption may be underestimated. Therefore, a system in which the mixing of the label with the soil pores is improved will result in greater accuracy of the pool dilution approach.

In this study, we used a novel open dual headspace system with field-relevant O_2 concentrations to incubate intact sandy clay loam agricultural topsoil and subsoil cores. This system was developed to answer the following question: *does the balance between soil N_2O production and consumption differ between soil depths and moisture contents in intact agricultural soil cores?* Following the ^{15}N - N_2O pool dilution (Wen et al., 2016; Yang et al., 2011) and Currie method (Currie, 1960) with SF_6 as a conservative tracer, the relative diffusivity (D_s/D_0), net N_2O emission, and gross N_2O emission and uptake rates were measured. We hypothesised that, (i) the rate of diffusion would decrease with soil depth and wetness due to greater soil density and lower porosity; (ii) despite higher N_2O and lower O_2 concentrations deeper in the soil, consumption of N_2O will be greater in the more

microbially active topsoil; and (iii) a WFPS above the critical level (ca. $\geq 60\%$; Bateman & Baggs, 2005) will increase N_2O consumption, whereas at a lower WFPS, N_2O consumption will be minimal.

2 | MATERIALS AND METHODS

2.1 | Soil collection and characterization

Sandy clay loam textured freely draining arable soil was collected from Abergwyngregyn, North Wales ($53^{\circ}14'29''$ N, $4^{\circ}01'15''$ W) in February 2020. The soil is classified as a Eutric Cambisol (WRB) or Typic Hapludalf (US Soil Taxonomy) and has a crumb structure because of high levels of earthworm bioturbation. This soil was chosen because it is a globally extensive temperate soil type and is common in agricultural production (WRB, 2014). Prior to collection, the field had been used for winter wheat (*Triticum aestivum*) production. Soil was collected from 6 randomly selected locations within the field from the topsoil (0–10 cm) and subsoil (50–60 cm), which were retained as 6 independent replicates. The latter soil depth was from below the plough layer and the field had no history of subsoiling. The latter depth was chosen as it was representative of the B horizon, assumed to be ‘undisturbed’ from mechanical soil management and provided enough distinction in soil characteristics from the topsoil cores. Two disturbed soil samples and three intact soil cores (using stainless steel rings of 53 mm outside diameter \times 50 mm height, 104 cm³ volume; steel from Complete Stainless Ltd., Glasgow, UK) were collected from each hole at each depth, excluding spare cores used for soil characterization. Soil cores were collected by lightly hammering in the steel rings at the appropriate soil depth and retrieving them, when the entire volume was filled, by carefully digging them out. The soil cores were then placed in plastic bags (but not sealed) in the field and stored at $<5^{\circ}C$ prior to use.

One of the sets of three soil cores per depth and hole were removed from their metal core rings, weighed and oven-dried ($105^{\circ}C$, 24 h) immediately after collection. The dry bulk density was determined by dividing the dry weight by the soil volume. WFPS was determined using the volumetric water content, particle density, and bulk density, using the following equation:

$$WFPS = \frac{B_d \cdot M_c}{1 - \frac{B_d}{P_d}} \cdot 100, \quad (1)$$

where the B_d is the dry bulk density ($g\ cm^{-3}$) and M_c is the moisture content ($g\ g^{-1}$) and their product is the volumetric water content ($cm^3\ cm^{-3}$). P_d is the particle

TABLE 1 Properties of the Eutric Cambisol topsoil (0–10 cm) and subsoil (50–60 cm) used for the study.

Properties	Topsoil 0–10 cm	Subsoil 50–60 cm
Sand (%) ^a	62.9 \pm 0.7	67.2 \pm 6.5
Silt (%) ^a	16.2 \pm 1.3	14.9 \pm 3.1
Clay (%) ^a	20.9 \pm 1.0	17.9 \pm 4.1
Dry bulk density ($g\ cm^{-3}$)	1.11 \pm 0.06	1.26 \pm 0.04
Porosity (%)	55.7 \pm 0.8	53.0 \pm 3.5
Organic C ($g\ C\ kg^{-1}$)	27.8 \pm 1.3	7.4 \pm 1.0
Total N ($g\ N\ kg^{-1}$)	3.4 \pm 0.1	1.5 \pm 0.1
C:N ratio	8.1 \pm 0.1	4.8 \pm 0.3
pH _{H2O}	6.8 \pm 0.06	6.8 \pm 0.03
EC ($\mu S\ cm^{-1}$)	1198 \pm 126	657 \pm 102
Extractable NH_4^+ ($mg\ N\ L^{-1}$)	0.08 \pm 0.02	0.09 \pm 0.03
Extractable NO_3^- ($mg\ N\ L^{-1}$)	41.1 \pm 6.0	22.4 \pm 5.2
Dissolved organic C ($mg\ C\ L^{-1}$)	12.6 \pm 1.3	4.3 \pm 1.8
Dissolved organic N ($mg\ N\ L^{-1}$)	4.9 \pm 2.1	0.6 \pm 0.4
Soil microbial biomass ($mg\ C\ kg^{-1}$)	74.0 \pm 3.7	42.9 \pm 1.4

Note: Values represent means \pm SEM ($n = 4$) and values are expressed on a dry soil weight equivalent where appropriate.

^aData from Sanchez-Rodriguez et al. (pers. comm.), $n = 4$.

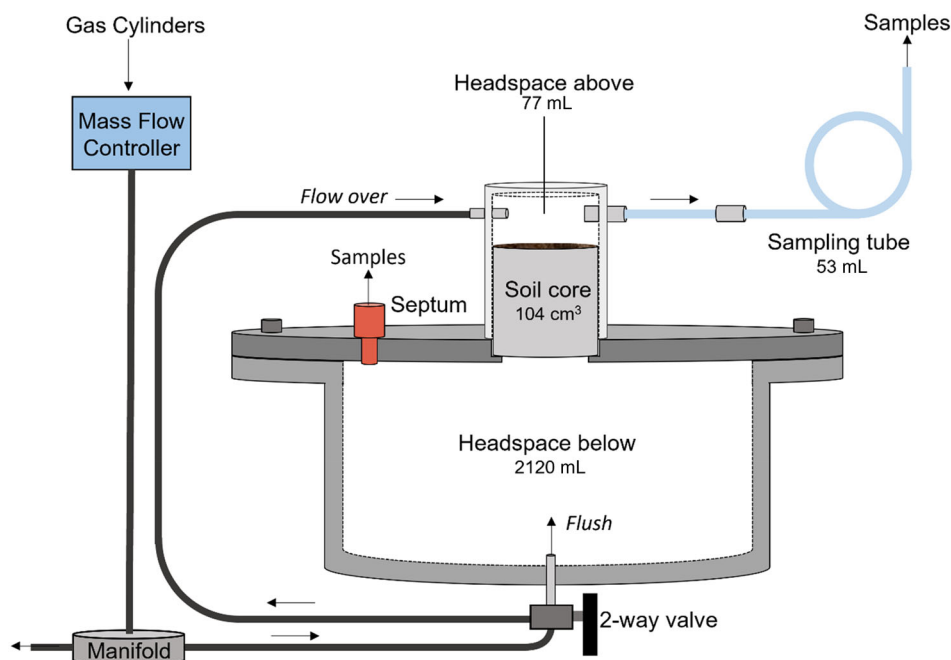
density, assumed at $2.65\ g\ cm^{-3}$. $1 - B_d/P_d$ is the total porosity ($cm^3\ cm^{-3}$).

5 g replicates of soil were extracted using 0.5 M K_2SO_4 at a ratio of 1:5 (w/v) on the same day the soil was collected. These were shaken at 200 rpm for 30 min and then centrifuged (14,000g, 10 min). The supernatant was then removed and frozen for ammonium (NH_4^+) and NO_3^- content determination by colourimetry, according to Mulvaney (1996) and Miranda et al. (2001), respectively, with a PowerWave XS Microplate Spectrophotometer (BioTek Instruments Inc., Winooski, VT). Dissolved organic C and N in the extracts was determined using a Multi N/C 2100/2100 analyser (AnalytikJena AG, Jena, Germany). Dissolved organic N was determined by subtracting inorganic N (NO_3^- and NH_4^+) from the total dissolved N. Soil EC and pH in water were determined in a 1:5 ratio (w/v) using a Jenway 4520 conductivity meter and a Hanna 209 pH meter (Hanna Instruments Ltd., Leighton Buzzard, UK), respectively. A summary of the initial soil properties is provided in Table 1.

2.2 | Experimental system

A specialized gas-flow-soil-core incubation system (DENitrification Incubation System [DENIS]; Cárdenas

FIGURE 1 The dual-headspace system used for incubating the soil cores in this study. The system can be placed in two different modes, 'flush' and 'flow over'. The former is where air flow from the gas cylinders is directed to enter via the headspace below the core, while the latter directs this air via the headspace above the soil core. All dimensions, materials and a photograph of the system can be found in the Supplementary Information (S1).



et al., 2003), allowing controlled environmental condition control (including O_2 concentration and temperature), was adapted for this study using custom-made lids used by Boon et al. (2013). The system, with 12 large individual stainless steel chambers (2120 mL), was modified to hold 53 mm wide soil cores with a lid and septum for direct gas application and sampling from a small headspace (77.2 mL) with a 3 m (4.8 mm ID, 53.4 mL) sampling tube (Figure 1). Details of the DENIS modification and a photograph are provided in the Supplementary Information (S1, Figure S1).

The gas flow from the O_2 and N_2 (see ratios in 2.4) cylinders into the system was adjusted via mass flow controllers (MFC) to achieve the desired flow rate and O_2 concentration, and then split evenly into each of the 12 incubation vessels via a manifold. A valve (Figure 1) enabled flow to be either directed to enter the large headspace below the intact soil cores ('flush mode') or to enter the small headspace on top of the intact soil cores ('flow over mode'). In both modes the gas exited via the sampling tube. The MFC was calibrated for all gases used in the experiment by measuring the flow 5 times at 10 flow rate settings with a bubble meter.

In this study, two gases were used to generate the 'flush' and 'flow over' the intact soil cores (Figure 1): an ECD-Grade N_2 cylinder and a grade zero O_2 cylinder (BOC; Linde plc, Guildford, UK). The N_2 cylinder and a compressed air line that was used for the 'flow over mode' both had SF_6 concentrations below atmospheric levels (i.e., <10 ppt). During pilot studies, we discovered that the SF_6 concentration in the O_2 cylinder was surprisingly high (ca. 6 ppb), which is about three orders of

magnitude greater than the concentration of atmospheric SF_6 (10.6 ppt). Therefore, we decided to use this as our source of SF_6 for the incubation.

^{15}N labelled N_2O was generated specifically for this experiment using the ammonium sulphate method described by Laughlin et al. (1997). This generates N_2O and N_2 at the same ^{15}N enrichment as the ammonium sulphate. The generated N_2O and N_2 were collected in evacuated exetainers (Labco Ltd., Lampeter, UK). N_2 was removed using the cryotrapping loops in a Sercon trace gas analyser (TG2, Sercon Ltd., Crewe, UK) so that the N_2O was trapped while the N_2 was flushed to waste. Once the N_2 had been removed, N_2O was collected in a Tedlar[®] gas sample bag from the outlet of the TG2. The contents of the Tedlar[®] bag were analysed for N_2O and N_2 concentration and enrichment using a Sercon trace gas analyser and Sercon 20:22 isotope ratio mass spectrometer (Sercon Ltd., Crewe, UK).

2.3 | Soil core preparation and installation

Soil cores from both depths were brought to either 50% or 70% WFPS for the incubation experiment. These WFPS were chosen as they are either side of the 60% WFPS threshold for N_2O production and N_2O produced is likely to be underpinned by different processes (Bateman & Baggs, 2005). Soil cores were brought to the desired weight for attaining a WFPS of 50% or 70% ($n = 6$ each) by adding distilled water (70% WFPS) or air-drying the approximate field moist soil (50% WFPS). To calculate

the difference in moisture content (ΔM_c) for achieving for the required WFPS (50% or 70%) in the incubation, the required WFPS level ($WFPS_R$; %) was multiplied by the total pore space volume (PS_v ; cm^3) as demonstrated in Equation (2). The moisture content of the core (M_{cc} ; cm^3) was then subtracted to obtain the difference in the soil core moisture to achieve the required WFPS.

$$\Delta M_c = \frac{WFPS_R \cdot PS_v}{100} - M_{cc}. \quad (2)$$

The water required to reach the desired WFPS level in the cores was pipetted onto the surface of the cores 24 h before installation in the incubation system. Where this water did not immediately infiltrate, it was done in stages so all the water was pipetted and it did not run down the sides of the core. Cores that required WFPS level reduction were air-dried and subsequently adjusted with additional water if they overshot the target (as described above). Cores that had not lost enough weight after air-drying overnight to meet the required WFPS were further dried in an incubator at 40°C (see Supplementary Information S3, for more information). Once all the cores had attained the target WFPS, they were installed randomly in the system (Figure 1). The inside edges of the top of the soil cores (ca. 2–4 mm) were carefully sealed with silicone grease to ensure no edge related diffusion effects. This was also done on the bottom of the soil cores, where drying had caused cores to slightly (<1 mm) shrink away from the metal core ring. A circular nylon mesh was placed in the lid groove before the cores were installed to prevent the soil from falling into a large headspace. The cores were then lightly tapped into the steel lids of the large headspaces of the incubation vessels using a mallet. The inside walls of the small headspace chambers and where they met the large headspace lids were also greased with silicone to ensure an airtight fit. This was confirmed by measuring gas flow through all 12 cores using a bubble flow meter.

2.4 | Soil core incubation

Soil cores were incubated in the dark, and the temperature in the laboratory was kept constant at 22°C for the 4–5 day incubation (depending on soil depth). As an acclimatization period, the soil cores were put into ‘flush mode’ at a flow rate of 5 mL min^{-1} core⁻¹ for ca. 18 h with an SF₆-containing (see Section 2.2) O₂:N₂ mixture. This mix was 20.9:100 and 13:100 O₂:N₂ for the 0–10 and 50–60 cm cores, respectively. The O₂ content of the mix was chosen by a fitted trend of a similar soil profile (Figure S3). The acclimatization period allowed the air-filled pore space to

attain an air mix representative of the soil core depths and for the accumulation of a reservoir of SF₆ tracer gas in the headspace below the soil core.

After the ‘flush mode’, the gas flow was momentarily stopped and the (high SF₆) O₂ cylinder was exchanged for a (ambient-SF₆) compressed air cylinder and the flow adjusted to maintain the same O₂:N₂ ratio. The flow was changed to ‘flow over mode’ by switching the valve below the large headspace to divert the gas to flow over the small headspace (Figure 1) and resumed at the same rate (ca. 5 mL min^{-1} vessel⁻¹) for the rest of the experiment. The vessels were left for ca. 4 h to remove the high SF₆ gas concentrations in the above core headspace from the ‘flush mode’. 60 mL of 30 atom% containing 85 and 100 ppm ¹⁵N-isotopically labelled N₂O was then syringe-injected into the 0–10 cm and 50–60 cm core large headspace vessels (below the intact soil cores) via the septum (Figure 1), achieving a ¹⁵N₂O headspace concentration below the soil core of 2.4 and 2.8 ppm, respectively. These represent the in situ concentrations of N₂O at the same field site between the two depths (ca. 30 cm; Figure S4). The flow rate was tested daily three times per core after sampling using a bubble meter, and these specific flow rates were used to calculate the fluxes.

2.5 | Gas sampling and analysis

Approximately 30 min after injection of the ¹⁵N₂O into the headspace below the intact soil cores, the large headspace was assumed to be mixed and the initial ‘ $t = 0$ ’ SF₆ (10 mL) and mass spectrometry (duplicate 12 mL) samples were taken using separate gas-tight 20 mL polypropylene syringes. The samples were assumed to be representative of the large headspace by filling and emptying the syringe three times into the headspace before a gas sample was taken. SF₆ samples were analysed immediately, while the duplicate samples for mass spectrometry were injected directly into 12 mL pre-evacuated (flushed with Helium and doubly evacuated) Exetainers® (Labco Ltd., Lampeter, UK). Below core headspace samples were taken daily for SF₆ analysis. Samples from the headspace below the soil core for mass spectrometry were taken at the start (day 1) and end of the incubation (day 3 or 4) so as to limit the removal of gas from the below core headspace. In addition, because of the ability to account for the gas pool from above the core headspace and SF₆ diffusion, a high temporal resolution was not required for pool dilution calculations. A total of 4% of the volume of gas in the headspace below the soil core was removed for analysis across the incubation period, which was factored into the gas concentration calculations. Headspace above the core were sampled (via the

sampling tube) for SF₆ and mass spectrometry (duplicate) analysis daily, with these always taken before headspace below the soil core samples. This was done by disconnecting the sampling tube (see Figure 1) from the headspace (to avoid creating negative pressure in the system and turbulent mixing with ambient air) and then connecting a syringe to the tube and taking samples before re-connecting the sampling tube. The volume of the sampling tube (53.4 mL) was sufficient to collect two samples (maximum of 24 mL) without diluting with ambient air, as was tested (Supplementary Information S2, Figure S2).

One of the two duplicate samples was analysed by analysed for N₂O and N₂ concentration and enrichment using a Sercon trace gas analyser and Sercon 20:22 isotope ratio mass spectrometer (Sercon Ltd., Crewe, UK), whereas the other was spare in case of analysis failure. Samples were stored for 8 months before analysis due to COVID-19 related restrictions to laboratory access and delays. Simultaneously, 12 mL N₂O standards (5 ppm; $n = 15$) were stored with the samples to track any loss of concentration across the storage period. After this period, the mean standard concentration of this stored 5 ppm standard was 4.34 ppm ± 0.07. The analysed concentrations were adjusted to compensate for losses during storage.

For the analysis of SF₆, the 10 mL samples were used to flush and fill a 1 mL loop that was then injected directly into a Shimadzu GC-8A (Shimadzu KK, Kyoto, Japan) equipped with an Electron Capture Detector (ECD) and adapted for the rapid and precise analysis of SF₆ in either the gas or water phase (Law et al., 1994). Separation of SF₆ from O₂ and N₂O was achieved by a 3 m by 1/8" stainless steel column packed with molecular sieve 5A. The system was calibrated daily using a six-point calibration curve to cover the large range of concentrations observed between the two gas reservoirs. Analytical precision was typically better than 1%, and the detection limit was close to 2 pptv.

2.6 | Diffusion coefficient (D_s) calculation

The natural logs of SF₆ concentration depletion in the vessels were plotted against time for each WFPS treatment and soil depth. The diffusion coefficient (D_s) was then calculated from the gradient of the depletion curve using Equation (3).

$$C = \frac{2h \exp(-D_s a_1^2 t / \epsilon)}{L(a_1^2 + h^2) + h}, \quad (3)$$

where, C is the concentration of gas in the chamber (g m⁻³); ϵ is total air-filled porosity (m³ of air m⁻³ soil);

L is the depth of the soil core (m); t is time (h); $h = \epsilon (a\epsilon_c)$, where $\epsilon_c = 1$, is the air content of the chamber (m³ of air m⁻³ chamber); a is the volume of the chamber per area of soil (m³ of air m⁻² soil). A plot of $\ln C$ against time becomes linear with slope $-D_s a_1^2 t / \epsilon$ for sufficiently large t . The value of a_1 can be found using the table in Rolston and Moldrup (2002). The relative diffusion (D_s/D_0) of gas was calculated using the diffusion rate of SF₆ in air, D_0 (0.093 m² s⁻¹; Rudolph et al., 1996).

2.7 | ¹⁵N-N₂O pool dilution calculation

The calculation of gross production and consumption of N₂O was done using the modified (Wen et al., 2016, 2017) ¹⁵N-N₂O pool dilution method developed by Yang et al. (2011) from von Fischer and Hedin (2002):

$$[^{14}\text{N}_2\text{O}]_t = \frac{F_{14} \cdot P}{k_{14} + k_l} - \left(\frac{F_{14} \cdot P}{k_{14} + k_l} - [^{14}\text{N}_2\text{O}]_0 \right) \cdot e^{-(k_{14} + k_l) \cdot (t - t_0)}, \quad (4)$$

$$[^{15}\text{N}_2\text{O}]_t = \frac{F_{15} \cdot P}{k_{15} + k_l} - \left(\frac{F_{15} \cdot P}{k_{15} + k_l} - [^{15}\text{N}_2\text{O}]_0 \right) \cdot e^{-(k_{15} + k_l) \cdot (t - t_0)}, \quad (5)$$

where the concentration of ¹⁴N₂O at time t ($[^{14}\text{N}_2\text{O}]_t$) is calculated as the product of the N₂O concentration (ppb) and the ¹⁴N-N₂O atom% (i.e., 100 - ¹⁵N-N₂O atom%); $[^{15}\text{N}_2\text{O}]_t$ is the concentration of ¹⁵N₂O at time t , calculated as the product of the N₂O concentration (ppb) and the ¹⁵N-N₂O atom% excess (assuming a ¹⁵N isotope composition of background N₂O of 0.3688 atom%; Yang et al., 2011); F_{14} and F_{15} are the ¹⁴N₂O (0.997) and ¹⁵N₂O (0.003) mole fractions of emitted N₂O, respectively; k_{14} and k_{15} are the first-order rate constants of ¹⁴N₂O and ¹⁵N₂O reduction to N₂, respectively, calculated using Equation (6) and the average literature value ($\alpha = 0.9924 \pm 0.0036$; Yang et al., 2011) for the stable N isotopic fractionation factors defined as $\alpha = k_{15}/k_{14}$; k_l is the first-order exponential decay constant for SF₆ concentrations over time and represents physical loss via diffusion and/or advection (von Fischer & Hedin, 2002), calculated using Equation (6); t is the time (h) when the headspace was sampled. The gross N₂O emission (ppb h⁻¹), P , was calculated as the sum of Equations (4) and (5) relative to their mole fractions, solved using MATLAB (MathWorks, Version R2022a, USA).

The first-order rate constants for ¹⁵N₂O (k_{15}) and SF₆ (k_l) were calculated using the following equation:

$$k = -\frac{\ln\left(\frac{C_t}{C_0}\right)}{t}, \quad (6)$$

where k is the first-order rate constant; C_t and C_0 are the concentrations (ppb) of the gas at sampling time t (h) and at $t = 0$, respectively. The rate constant for $^{14}\text{N}_2\text{O}$, k_{14} , was calculated by solving $\alpha = k_{15}/k_{14}$, as described above.

The net N_2O emission from the flow-through small headspace was calculated as follows:

$$F = t \cdot f \cdot (C_{\text{out}} - C_{\text{in}}), \quad (7)$$

where F is the flux (ppb h^{-1}); t is the time (h) the sample is representative of; f is the flow rate of air through the headspace (L h^{-1}) and C_{out} and C_{in} are the concentrations of N_2O leaving and entering the headspace (ppb), respectively. The results from Equation (7) were then averaged and divided by the total incubation time to give a net flux (ppb h^{-1}) per incubation vessel.

The net emission (Equation 7) and gross production (Equations 6 and 7) N_2O rates were then converted to $\mu\text{g N kg}^{-1} \text{h}^{-1}$ using Equation (8).

$$F_E = \frac{F \cdot V_h}{10^{12}} \cdot \frac{p}{R \cdot (T + 273)} \cdot \frac{28}{W_d} \cdot 10^9, \quad (8)$$

where F_E is either the net emission or gross production of N_2O ($\mu\text{g N kg}^{-1} \text{h}^{-1}$), F is the net or gross emission of N_2O flux in ppb h^{-1} ; V_h is the headspace volume (L); R is the ideal gas constant ($8.314 \text{ J K}^{-1} \text{ mol}^{-1}$); p is the pressure (Pa); T is the incubation temperature ($^{\circ}\text{C}$) and 273 is the conversion constant to Kelvin; 28 is the molecular weight of N in N_2O (g mol^{-1}); W_d is the dry weight of the soil cores (g); 10^{12} and 10^9 are unit conversion factors. Gross N_2O consumption was then calculated as the difference between the gross N_2O production and net N_2O emission (Yang et al., 2011).

2.8 | Statistical analysis

All data analyses were performed using R (R Core Team, 2017), with figures made using the R package 'ggplot2' (Wickham, 2016). Data were assessed for test assumptions by using the Shapiro–Wilk test ($p > 0.05$) for normality, and Levene's test for homoscedasticity ($p < 0.05$) as well as assessing the qqplots and the residual versus fitted plots. The difference in mean small headspace versus mean large headspace SF_6 fluxes was tested with a Welch Two Sample t -test. Differences in relative diffusivity were tested individually by depth and WFPS, using a Welch two-sample t -test. Difference in fluxes with depth and WFPS were tested using 2-way ANOVAs. Data that did not meet assumptions were log or square root transformed to pass the Shapiro–Wilk and Levene's tests.

3 | RESULTS

3.1 | Relative diffusivity

As a test to ensure the SF_6 flux results from the small headspace and the depletion of SF_6 from the large headspace corresponded with each other, the fluxes were plotted against each other (Figure 2). The proximity of the data to the $x = y$ line demonstrate that they correspond well with each other. This is confirmed by the lack of a statistical difference between the fluxes from the small and large headspaces ($p = 0.62$). The linear trendline ($y = 1.26x - 0.29$) explained most of the variation in the data ($R^2 = 0.96$) but its deviation from the $x = y$ line highlights that the mean measured headspace below the soil core flux was overall 16.3% lower than that measured in the headspace above the soil core. While the cores at 70% WFPS ($R^2 = 0.55$; $y = 0.92x + 0.46$) more closely aligned with the $x = y$ 1:1 line, substantially more variation was explained by the line for the 50% WFPS cores ($R^2 = 0.98$; $y = 1.21x + 0.54$).

The differences in relative diffusivity (D_s/D_0) in the top- and subsoil cores at 50% and 70% WFPS can be seen in Figure 3. In the 0–10 cm depth cores, the diffusivity was significantly lower (79% lower; $p < 0.001$) at 70% WFPS than when incubated at 50% WFPS. A similar trend was found for the 50–60 cm depth soil cores, where the diffusivity was significantly lower (81% lower; $p < 0.001$) at 70% WFPS than when incubated at 50% WFPS. Thus, the overall effect of WFPS on gas diffusivity was significant ($p < 0.001$), while depth the core was taken from was not. While the 50–60 cm cores did have 12% and 21% lower relative diffusivities compared to the 0–10 cm cores at 50% and 70% WFPS, respectively, these differences were not significant ($p = 0.54$).

3.2 | Gross N_2O emission and uptake

The 0–10 cm depth soil cores produced 186% more gross N_2O at 50% WFPS ($1.03 \pm 0.46 \mu\text{g N kg}^{-1} \text{ha}^{-1}$) than at 70% WFPS ($0.36 \pm 0.12 \mu\text{g N kg}^{-1} \text{ha}^{-1}$). Similarly, the 50–60 cm depth cores produced 69% more gross N_2O at 50% WFPS ($0.59 \pm 0.04 \mu\text{g N kg}^{-1} \text{ha}^{-1}$) than at 70% WFPS ($0.35 \pm 0.04 \mu\text{g N kg}^{-1} \text{ha}^{-1}$). As such, the overall effect of WFPS on gross N_2O production was significant ($p = 0.028$; Figure 4a). However, the overall effect of soil depth on gross N_2O production was not significant ($p = 0.70$), despite the 0–10 cm depth cores ($0.69 \pm 0.29 \mu\text{g N kg}^{-1} \text{ha}^{-1}$) producing 47% more gross N_2O than the 50–60 cm cores ($0.47 \pm 0.04 \mu\text{g N kg}^{-1} \text{ha}^{-1}$), overall. This was driven by differences between the 50% WFPS cores at different depths, as there was only a 2%

FIGURE 2 The fluxes of SF₆ (means \pm SEM; $n = 6$) from the headspace above versus the headspace below soil cores from the 0–10 and 50–60 cm soil depths at 50% and 70% water-filled pore space. The dashed line represents the best fit for the flux data ($R^2 = 0.96$; $y = 1.26x - 0.29$) and the solid line represents the $y = x$. Note that the axes are logarithmic.

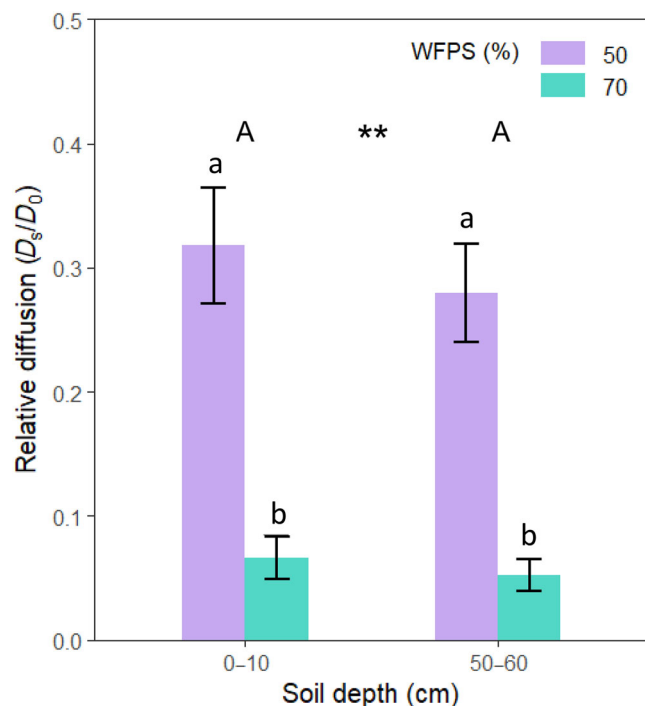
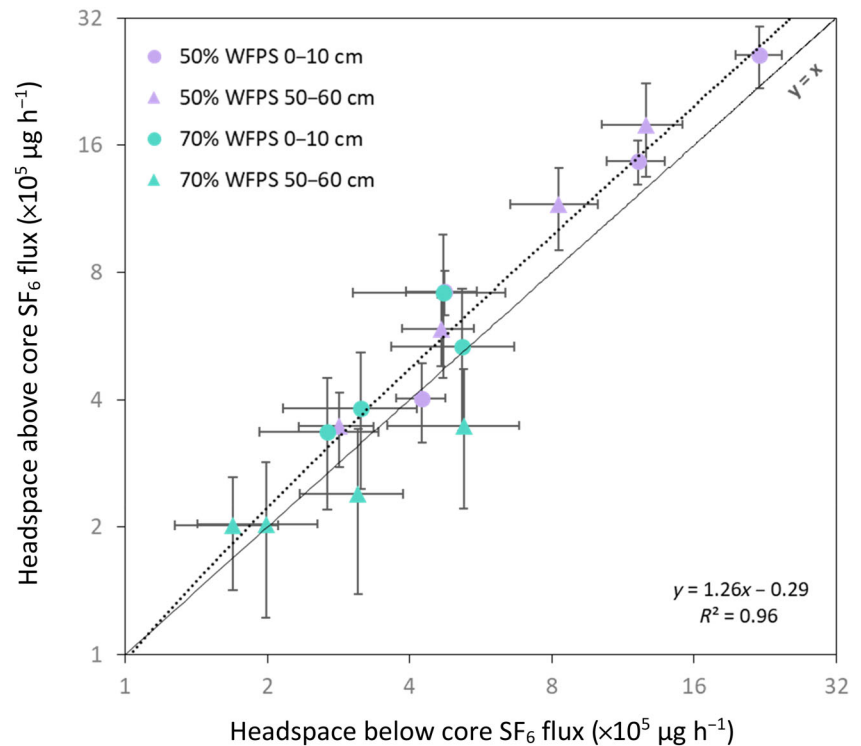


FIGURE 3 The mean (\pm SEM) relative diffusivity (D_s/D_0) of intact top- and subsoil cores at two different levels of water-filled pore space (WFPS, %; $n = 6$). Different letters represent statistical difference of means between soil depths (upper-case) and between soil depth and WFPS (lower-case) at $p < 0.05$. Asterisks represent statistical difference in overall WFPS means at $p < 0.001$ (**); $p < 0.01$ (**); $p < 0.05$ (*) and $p > 0.05$ (-).

difference in gross N₂O production between the depths at 70% WFPS. For gross N₂O uptake, 216% more N₂O was taken up in the soil at 50% ($0.98 \pm 0.46 \mu\text{g N kg}^{-1} \text{ha}^{-1}$) WFPS than at 70% WFPS ($0.31 \pm 0.12 \mu\text{g N kg}^{-1} \text{ha}^{-1}$) in the 0–10 cm soil cores. Following a similar trend in the 50–60 cm cores, 69% more N₂O was taken up in the soil at 50% WFPS ($0.54 \pm 0.03 \mu\text{g N kg}^{-1} \text{ha}^{-1}$) than at 70% WFPS ($0.32 \pm 0.04 \mu\text{g N kg}^{-1} \text{ha}^{-1}$). The overall effect of WFPS on gross N₂O uptake was significant ($p = 0.036$; Figure 4b). There was only a 4% difference in gross N₂O uptake between the depths at 70% WFPS, whereas 49% more N₂O was taken up by the 0–10 cm soil cores ($0.64 \pm 0.29 \mu\text{g N kg}^{-1} \text{ha}^{-1}$) compared to the 50–60 cm cores ($0.43 \pm 0.04 \mu\text{g N kg}^{-1} \text{ha}^{-1}$) at 50% WFPS. Despite this, there was no overall effect of soil depth on gross N₂O uptake ($p = 0.97$).

3.3 | Net N₂O emission

Net emissions of N₂O were overall higher in the cores at 50% WFPS ($0.05 \pm 0.01 \mu\text{g N kg}^{-1} \text{ha}^{-1}$) than at 70% ($0.04 \pm 0.001 \mu\text{g N kg}^{-1} \text{ha}^{-1}$, $p = 0.042$). This difference was driven by the 41% lower emissions from the 70% cores at 50–60 cm ($0.03 \pm 0.002 \mu\text{g N kg}^{-1} \text{ha}^{-1}$; Figure 4c) compared with the 0–10 cm cores at the same WFPS ($0.05 \pm 0.01 \mu\text{g N kg}^{-1} \text{ha}^{-1}$). In the 50–60 cm cores, the emissions from the 50% WFPS ($0.04 \pm 0.002 \mu\text{g N kg}^{-1} \text{ha}^{-1}$) treatment were 52% higher than

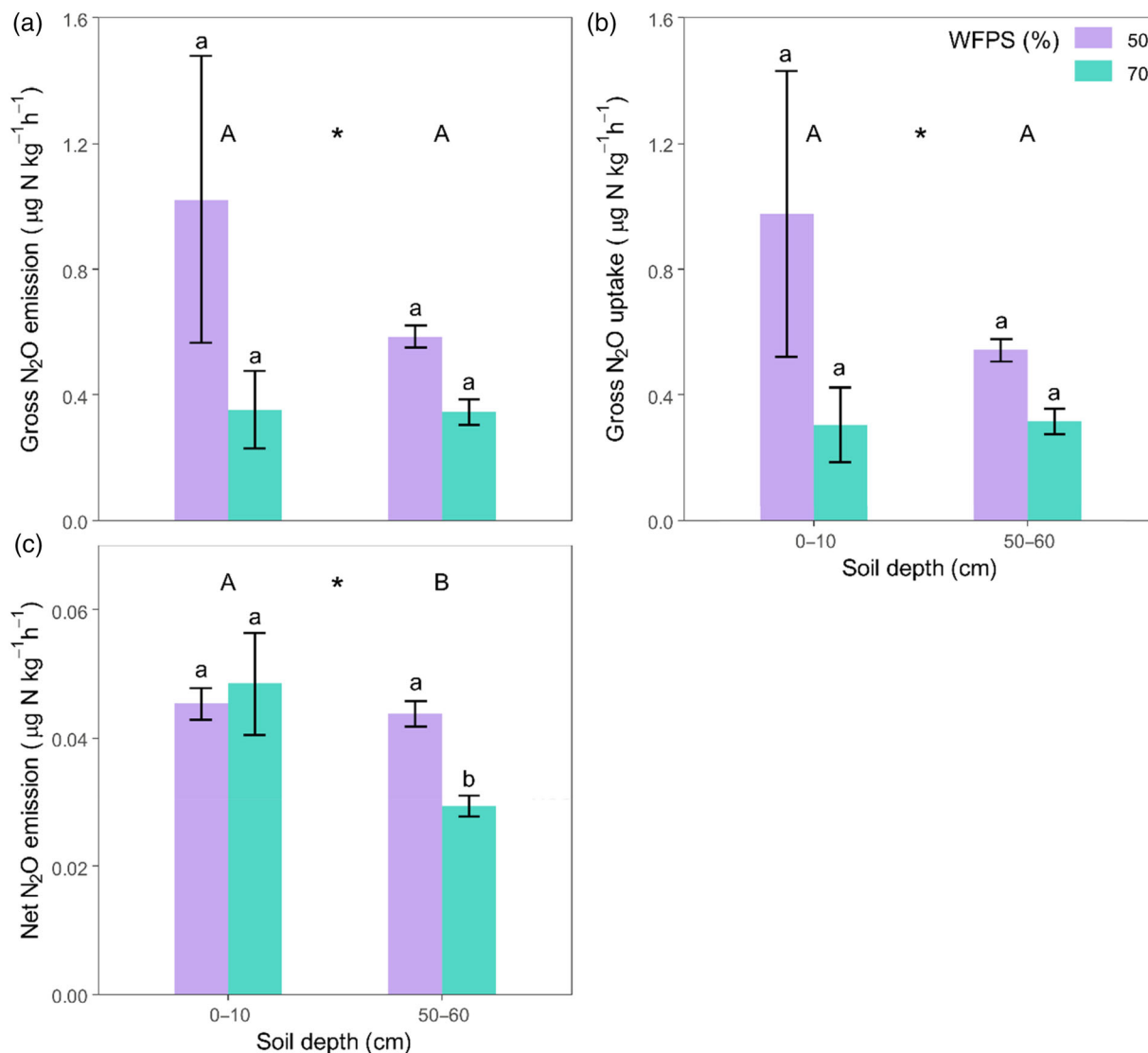


FIGURE 4 The gross N₂O emission (i); gross N₂O uptake (ii), and; net N₂O emission (iii) (means ± SEM; $n = 6$) in intact 0–10 and 50–60 cm soil cores at 50% and 70% water-filled pore space (WFPS) measured by the ¹⁵N-N₂O pool dilution method. Different letters represent statistical difference of means between soil depths (upper-case) and between soil depth and WFPS (lower-case) at $p < 0.05$. Asterisks represent statistical difference in overall WFPS means at $p < 0.001$ (***); $p < 0.01$ (**); $p < 0.05$ (*) and $p > 0.05$ (-).

in the 70% WFPS ($0.03 \pm 0.002 \mu\text{g N kg}^{-1} \text{ha}^{-1}$) treatment, but 5% lower than from the 70% WFPS cores. Overall, the 0–10 cm soil cores had 30% higher net N₂O emissions ($0.05 \pm 0.01 \mu\text{g N kg}^{-1} \text{h}^{-1}$) compared to the deeper soil cores ($0.04 \pm 0.002 \mu\text{g N kg}^{-1} \text{h}^{-1}$; $p = 0.014$; Figure 4c).

4 | DISCUSSION

4.1 | Soil diffusivity

While the agreement between the small and large headspace SF₆ fluxes was good (Figure 2), we attribute the

overall higher fluxes in the headspace above the core compared to the headspace below the core is likely due to a technical factors. Because of the sampling of the headspaces above the cores prior to those below (to avoid any negative pressure influencing the above core headspace sample), there was a 1–2 h time delay between these, as the samples needed to be injected directly into the GC. Considering the exponential depletion of SF₆ from the headspace below the cores, this time lag would translate to slightly different fluxes. Therefore, we believe the difference between the calculated fluxes is predominantly due to the delay in above core headspace samples. We believe the nature of the fit to be within an acceptable range of error for the relationship between the small and

large headspaces to produce meaningful results from the ^{15}N - N_2O pool dilution.

The relative diffusivity values in Figure 2 (0.024–0.480) are consistent with the expected values for the exponential increase in D_s/D_0 with increasing air-filled pore porosity for soils with different overall pore architectures (Hashimoto & Komatsu, 2006) and using different measuring techniques (Allaire et al., 2008). The hypothesis that soil diffusion would be reduced by both increasing depth and WFPS was only partly confirmed (Figure 3). As expected, the highest WFPS in the soil reduced gas diffusivity of the soil substantially, but the different inherent physical soil characteristics (bulk density, porosity, and texture; Table 1) of the cores did not affect the D_s/D_0 of the soil when at the same WFPS. Fujikawa and Miyazaki (2005) found that D_s/D_0 increases with higher bulk density which they attributed to lower total porosity via the change in shape and size of pores which can be assumed to restrict gas movement, consistent with other studies (Balaine et al., 2013; Currie, 1984). However, these studies were all done on sieved and repacked soil which would create a more homogenous soil pore structure and can cause significant errors in determining the ‘true’ D_s/D_0 (Allaire et al., 2008). The inherent pore structure and preferential flow pathways (i.e., macropores, soil pipes and cracks) were preserved in the cores (although edge-related diffusion was avoided by sealing these) and this heterogeneity is a primary factor driving gas flow and is very important for studying gas diffusion (Allaire et al., 2008; Chamindu Deepagoda et al., 2019; Guo & Lin, 2018). However, no difference in D_s/D_0 between intact soil cores at a range of depths, bulk densities and porosities have also been observed (Chamindu Deepagoda et al., 2019). We attribute this lack of difference between depths to the presence of natural macropores, pipes and preferential flow paths that create similarities in the diffusivity of gas through the soil and the differences in soil physical properties was not sufficient to drive differences in D_s/D_0 .

4.2 | Gross N_2O uptake

Evidence for N_2O consumption by soils is extensive in the literature (see review by Chapuis-Lardy et al., 2007). In our study, we report gross N_2O -N uptake rates ranging from 0.03 to 2.79 $\mu\text{g N kg}^{-1} \text{h}^{-1}$ (Figure 4b) which is a similar range to that measured by others in similar agricultural soils (Clough et al., 2006; Luo et al., 2022; Wen et al., 2016). N_2O consumption rates, in our study, correlated closely with production rates, which is consistent with other studies (Wen et al., 2016; Yang et al., 2011; Yang & Silver, 2016), suggesting that consumption

increased proportionally with N_2O production (Figure 4a,b). These results uncovered a high potential for N_2O uptake that would have been masked by higher N_2O production had only the latter been measured.

The hypothesis that the uptake of N_2O would be greater in the more microbially-active topsoil compared to the subsoil was rejected (Figure 4b). While the uptake rate was highest in the topsoil cores at 50% WFPS, there was no statistical difference between depths. This is despite there being a lower microbial biomass (indicating size of the microbial community; Table 1) and a lower abundance of denitrification (*nirK*, *nirS*) and complete denitrification (*nosZ*) gene copies in the subsoil (indicating denitrification potential of the microbial community; Table S1). Scaling the magnitude of N_2O uptake relative to the size and denitrification potential of the soil microbial community, it was much greater in the subsoil compared to the topsoil. Care should be taken with this interpretation as microbial biomass size does not necessarily indicate the activity of denitrifiers, and gene abundance does not necessarily link to process rates as discussed in a meta-analysis conducted by Rocca et al. (2015).

The reduction of N_2O to N_2 can be considerable in the subsoil, dependent on a combination of inherent soil characteristics (C, NO_3^-) and physical conditions (WFPS, O_2 concentration, diffusivity) (Clough et al., 1999, 2005; Semedo et al., 2020). Within the topsoil the organic C, total N, dissolved organic C, dissolved organic N and extractable NO_3^- were greater than that found in the subsoil (Table 1). Thus, labile C and N substrate supply likely differed between depths during the course of the experiment. As discussed previously, NO_3^- can outcompete N_2O as the terminal electron acceptor during complete denitrification (Chapuis-Lardy et al., 2007), potentially contributing to differences in N_2O uptake rates between depths. In addition, the cores in this study were incubated at an O_2 content similar to their in situ levels—which was 20.9% and 13% in the topsoil and subsoil incubations. Due to 38% less O_2 in the subsoil cores, the formation of semi-anaerobic and full anaerobic conditions required for N_2O production and consumption would be more easily achieved. This is supported by others that found increased denitrification when O_2 was restricted (Patureau et al., 1996; Schlüter et al., 2018), which would explain the lack of difference in gross N_2O uptake between soil depths.

Higher WFPS decreases the diffusion of N_2O produced in the soil to the surface and increases its residence time allowing for higher potential of complete denitrification of N_2O to N_2 (Balaine et al., 2013; Chamindu Deepagoda et al., 2019). While the diffusion rate did decrease with greater WFPS (Figure 3), this did not

produce a difference between the N₂O uptake rates of the soil cores incubated at different WFPS levels. In fact, the 50% WFPS cores had higher consumption rates. Therefore, we rejected our final hypothesis that N₂O uptake would be higher with increasing WFPS.

N₂O consumption is generally expected to occur under conditions of low N availability and high soil moisture (Chapuis-Lardy et al., 2007). While there is extensive literature that suggests there is a high WFPS 'critical threshold' at which consumption predominantly takes place (ca. >60%–80%; Bateman & Baggs, 2005; Chamindu Deepagoda et al., 2019; Davidson, 1991), there are studies that have found no differences or even an increase in N₂O uptake with lower WFPS (Goldberg & Gebauer, 2009; Khalil et al., 2002; Rosenkranz et al., 2006; Wu et al., 2013) and low N (Wang et al., 2018). A possible explanation for N₂O consumption in drier soil is greater diffusivity allowing N₂O present in air or headspace to diffuse to the denitrification site, where in the absence of NO₃⁻, N₂O may be used as an electron acceptor for denitrification (Chapuis-Lardy et al., 2007). Bazylnski et al. (1986) demonstrated this in isolated denitrifier growth using only N₂O as an electron acceptor. However, because of the presence of NO₃⁻ in the top- and subsoil (Table 1) this is unlikely to contribute substantially. A possible alternative pathway is aerobic nitrate reduction, which is the bacterial reduction of NO₃⁻ in aerobic conditions that can occur independently of denitrification gas-producing reactions and is an underappreciated nitrate sink according to Roco et al. (2016). However, despite 84% more NO₃⁻ in the topsoil compared to the subsoil (Table 1), no significant difference was measured between cores from these depths suggesting that this may not have been the primary mechanism. Without information on the changes in N pools it is not possible to determine the occurrence of this process. However, it suggests that substantial N₂O consumption in our study could be driven directly and/or indirectly by aerobic processes rather than anaerobic denitrification processes (Wang et al., 2018; Wu et al., 2013). If this is the case and anaerobic microsites were not an important location for denitrification in this study, the calculated gross N₂O production and consumption fluxes may be more accurate than expected from the pool dilution results. This is because the ¹⁵N-N₂O pool dilution method does not allow for accurate measurement of gross production and consumption of N₂O in situations most likely to be occurring within anaerobic microsites. These are when (i) N₂O produced is immediately consumed within the cells of denitrifiers, and (ii) produced N₂O diffuses out of denitrifiers and is taken up by other microbes without mixing with the ¹⁵N₂O label during the measurement period (Wen et al., 2016).

Due to the 58% smaller volumes of the cores in this study compared to Wen et al. (2016), these processes may have been less likely to occur due to shorter diffusion distances reducing the time N₂O spent in the soil and therefore the potential for its consumption in microsites.

4.3 | Gross N₂O emission

Gross N₂O emission rates varied from 0.056 to 2.83 μg N kg⁻¹ h⁻¹ (Figure 4a), which is within the range of measurements reported in other studies (Clough et al., 2006; Luo et al., 2022; Wen et al., 2016). These rates may be low as N₂O can be lost rapidly (hours) after wetting (Barrat et al., 2022; Smith & Tiedje, 1979). As the cores were brought to the desired WFPS ca. 18 h before the incubation, they may have already lost substantial soil N prior to incubation.

N₂O production is driven by microbial denitrification and nitrification in the soil under partially anaerobic and aerobic conditions (Chapuis-Lardy et al., 2007; Diba et al., 2011). The dominating process has been found to change from nitrification to denitrification at WFPS of 60%–70% (Bateman & Baggs, 2005; Pihlatie et al., 2004). This would suggest that the N₂O produced in the 50% and 70% WFPS cores was predominantly from nitrification or denitrification, respectively. However, these may occur in the soil simultaneously (Bateman & Baggs, 2005; Pihlatie et al., 2004). Denitrification is a common source of N₂O in many agricultural soils, and the close coupling between gross emission and uptake of N₂O as found in this study (Figure 4a,b), suggests denitrification was the dominant process (Chapuis-Lardy et al., 2007; Wen et al., 2016). According to Davidson (1991), N₂O production is greatest when at or near field capacity (ca. 60% WFPS) as nitrification and denitrification rates are comparable sources of N₂O occurring simultaneously. Therefore, a higher gross N₂O emission in the soil cores at 50% WFPS could be explained by simultaneous denitrification and nitrification producing N₂O. Nevertheless, we lack information to be able to source partition the N₂O generated in this study. Recent advances in N₂O isotopomer measurements are shedding light on microbial source partitioning of N₂O, for example, Stuchiner and von Fischer (2022b) demonstrate denitrification was the predominant N₂O production pathway in soils ranging from 50% to 95% WFPS and Harris et al. (2021) found that the proportion of N₂O from denitrification did not decrease under even very low WFPS.

Gross emission rates were not different with depth in this study (Figure 4a). Emission rates of N₂O have been observed to be higher in subsoil than in topsoil under certain conditions (Goldberg et al., 2008; Müller et al., 2004;

Shcherbak & Robertson, 2019). This may be due to denser, deeper soils becoming anaerobic more quickly as a result of a restriction in diffusivity and lower pore volume (Berisso et al., 2013). As the subsoil cores were incubated with almost 38% less O₂ than the topsoil, the formation of semi-anaerobic and full anaerobic conditions required for N₂O production would be more easily achieved. Therefore, despite higher biological N₂O production potential in the topsoil (Table 1), it would suggest that physical N₂O-promoting conditions in the subsoil can match this potential.

4.4 | Net N₂O emission

Net emissions from the soil cores varied between 0.025–0.084 µg N kg⁻¹ h⁻¹ (Figure 4c). This low emission rate is expected from an unfertilized, low N arable soil (Table 1; Wen et al., 2016). The net N₂O emission decreased with soil depth which is primarily due to the low rate from the 70% WFPS 50–60 cm cores (Figure 4c). This trend reflects the gross N₂O uptake and emission in the soil, as the net emission is the gross consumption subtracted from the gross emission.

5 | CONCLUSIONS

Using a novel dual-headspace system for soil core incubation, we demonstrated that this method is reliable for measuring fluxes both above and below a soil core at controlled O₂ concentration and for applying the ¹⁵N-N₂O pool dilution method. The fluxes measured from this system all fall within previously measured ranges measured in the field. We believe using a headspace both above and below the soil core is better than a single headspace approach as it is better placed to replicate the movement of gas through the soil and better mix gas from the reservoir with soil air, although this will require comparative testing. We provide evidence that the relative diffusivity of gas within intact soil cores does not differ with soil depth, likely because preferential flow pathways are preserved. This contrasts with studies that use sieved and repacked cores which allow for more equal mixing of labelled and non-labelled isotope pools, but do not represent or measure true soil diffusivity. Gross N₂O production and consumption rates did not differ with depth but were higher in the 50% WFPS cores. We attribute this to aerobic denitrification and simultaneous denitrification and nitrification for N₂O consumption and production, respectively. We provide further evidence to challenge the hypothesis that only wet soils play a crucial role in N₂O production, consumption, and net emissions. In

addition, we challenge the notion that only soils with net negative emissions experience substantial N₂O consumption rates. The results from this study provide a novel application of the ¹⁵N-N₂O pool dilution method and important evidence of N₂O production and consumption fluxes in low-N status, arable soil at different depths.

AUTHOR CONTRIBUTIONS

Erik S. Button, Laura M. Cárdenas, David R. Chadwick, and David L. Jones conceived the study. Erik S. Button conducted the experiments and wrote the manuscript, with specialist technical support from Philip D. Nightingale and Elizabeth R. Dixon. Karina A. Marsden supported Erik S. Button with the pool dilution calculations and interpretation. All authors reviewed the manuscript.

ACKNOWLEDGEMENTS

This work was supported by the FLEXIS (Flexible Integrated Energy Systems) programme, an operation led by Cardiff University, Swansea University and the University of South Wales and funded through the Welsh European Funding Office (WEFO). Rothamsted Research is supported by the Biotechnology and Biological Sciences Research Council (BBSRC, grants BBS/E/C/000I0310 and BBS/E/C/000I0320). The authors would like to thank Plymouth Marine Laboratory for the loan of the SF₆ GC. Sincere thanks also to Alan Jones for his excellent engineering advice and work; Lucy Greenfield for helping with the fieldwork; Nadine Loick and Neil Donovan for their technical support; Alex Boon for his help with the diffusion calculations and Marife Corre for her help with the pool dilution calculations. We thank the anonymous reviewers for their careful reading of the manuscript and their many insightful comments and suggestions.

DATA AVAILABILITY STATEMENT

The data that support the findings of this study are available from the corresponding author upon reasonable request.

ORCID

Erik S. Button  <https://orcid.org/0000-0001-5153-6022>

REFERENCES

- Allaire, S. E., Lafond, J. A., Cabral, A. R., & Lange, S. F. (2008). Measurement of gas diffusion through soils: Comparison of laboratory methods. *Journal of Environmental Monitoring*, 10, 1326–1336. <https://doi.org/10.1039/b809461f>
- Almaraz, M., Wong, M. Y., & Yang, W. H. (2020). Looking back to look ahead: A vision for soil denitrification research. *Ecology*, 101, 1–10. <https://doi.org/10.1002/ecy.2917>

- Balaine, N., Clough, T. J., Beare, M. H., Thomas, S. M., Meenken, E. D., & Ross, J. G. (2013). Changes in relative gas diffusivity explain soil nitrous oxide flux dynamics. *Soil Science Society of America Journal*, *77*, 1496–1505. <https://doi.org/10.2136/sssaj2013.04.0141>
- Barrat, H. A., Clark, I. M., Evans, J., Chadwick, D. R., & Cardenas, L. (2022). The impact of drought length and intensity on N cycling gene abundance, transcription and the size of an N₂O hot moment from a temperate grassland soil. *Soil Biology and Biochemistry*, *168*, 108606. <https://doi.org/10.1016/j.soilbio.2022.108606>
- Bateman, E. J., & Baggs, E. M. (2005). Contributions of nitrification and denitrification to N₂O emissions from soils at different water-filled pore space. *Biology and Fertility of Soils*, *41*, 379–388. <https://doi.org/10.1007/s00374-005-0858-3>
- Bazylnski, D. A., Soohoo, C. K., & Hollocher, T. C. (1986). Growth of *Pseudomonas aeruginosa* on nitrous oxide. *Applied and Environmental Microbiology*, *51*, 1239–1246. <https://doi.org/10.1128/aem.51.6.1239-1246.1986>
- Berisso, F. E., Schjønning, P., Keller, T., Lamandé, M., Simojoki, A., Iversen, B. V., Alakukku, L., & Forkman, J. (2013). Gas transport and subsoil pore characteristics: Anisotropy and long-term effects of compaction. *Geoderma*, *195–196*, 184–191. <https://doi.org/10.1016/j.geoderma.2012.12.002>
- Blagodatsky, S., & Smith, P. (2012). Soil physics meets soil biology: Towards better mechanistic prediction of greenhouse gas emissions from soil. *Soil Biology and Biochemistry*, *47*, 78–92. <https://doi.org/10.1016/j.soilbio.2011.12.015>
- Boon, A., Robinson, J. S., Nightingale, P. D., Cardenas, L., Chadwick, D. R., & Verhoef, A. (2013). Determination of the gas diffusion coefficient of a peat grassland soil. *European Journal of Soil Science*, *64*, 681–687. <https://doi.org/10.1111/ejss.12056>
- Boyer, E. W., Alexander, R. B., Parton, W. J., Li, C., Butterbach-Bahl, K., Donner, S. D., Skaggs, R. W., & Del Grosso, S. J. (2006). Modeling denitrification in terrestrial and aquatic ecosystems at regional scales. *Ecological Applications*, *16*, 2123–2142. [https://doi.org/10.1890/1051-0761\(2006\)016\[2123:MDITAA\]2.0.CO;2](https://doi.org/10.1890/1051-0761(2006)016[2123:MDITAA]2.0.CO;2)
- Butterbach-Bahl, K., Baggs, E. M., Dannenmann, M., Kiese, R., & Zechmeister-Boltenstern, S. (2013). Nitrous oxide emissions from soils: How well do we understand the processes and their controls? *Philos. Transactions of the Royal Society B: Biological Sciences*, *368*, 20130122. <https://doi.org/10.1098/rstb.2013.0122>
- Cárdenas, L. M., Hawkins, J. M. B., Chadwick, D., & Scholefield, D. (2003). Biogenic gas emissions from soils measured using a new automated laboratory incubation system. *Soil Biology and Biochemistry*, *35*, 867–870. [https://doi.org/10.1016/S0038-0717\(03\)00092-0](https://doi.org/10.1016/S0038-0717(03)00092-0)
- Chamindu Deepagoda, T. K. K., Jayarathne, J. R. R. N., Clough, T. J., Thomas, S., & Elberling, B. (2019). Soil-gas diffusivity and soil-moisture effects on N₂O emissions from intact pasture soils. *Soil Science Society of America Journal*, *83*, 1032–1043. <https://doi.org/10.2136/sssaj2018.10.0405>
- Chapuis-Lardy, L., Wrage, N., Metay, A., Chotte, J. L., & Bernoux, M. (2007). Soils, a sink for N₂O? A review. *Global Change Biology*, *13*, 1–17. <https://doi.org/10.1111/j.1365-2486.2006.01280.x>
- Clough, T. J., Jarvis, S. C., Dixon, E. R., Stevens, R. J., Laughlin, R. J., & Hatch, D. J. (1999). Carbon induced subsoil denitrification of ¹⁵N-labelled nitrate in 1 m deep soil columns. *Soil Biology and Biochemistry*, *31*, 31–41. [https://doi.org/10.1016/S0038-0717\(98\)00097-2](https://doi.org/10.1016/S0038-0717(98)00097-2)
- Clough, T. J., Kelliher, F. M., Wang, Y. P., & Sherlock, R. R. (2006). Diffusion of ¹⁵N-labelled N₂O into soil columns: A promising method to examine the fate of N₂O in subsoils. *Soil Biology and Biochemistry*, *38*, 1462–1468. <https://doi.org/10.1016/j.soilbio.2005.11.002>
- Clough, T. J., Sherlock, R. R., & Rolston, D. E. (2005). A review of the movement and fate of N₂O in the subsoil. *Nutrient Cycling in Agroecosystems*, *72*, 3–11. <https://doi.org/10.1007/s10705-004-7349-z>
- Currie, J. A. (1960). Gaseous diffusion in porous media part 1—A non-steady state method. *British Journal of Applied Physics*, *11*, 314–317. <https://doi.org/10.1088/0508-3443/11/8/302>
- Currie, J. A. (1984). Gas diffusion through soil crumbs: The effects of wetting and swelling. *Journal of Soil Science*, *34*, 217–232. <https://doi.org/10.1111/j.1365-2389.1983.tb01029.x>
- Davidson, E. A. (1991). Fluxes of nitrous oxide and nitric oxide from terrestrial ecosystems. In J. E. Rogers, & W. B. Whitman (Eds.), *Microbial production and consumption of greenhouse gases: Methane, nitrogen oxides, and halomethanes* (pp. 219–235). American Society for Microbiology.
- Davidson, E. A., Ishida, F. Y., & Nepstad, D. C. (2004). Effects of an experimental drought on soil emissions of carbon dioxide, methane, nitrous oxide, and nitric oxide in a moist tropical forest. *Global Change Biology*, *10*, 718–730. <https://doi.org/10.1111/j.1529-8817.2003.00762.x>
- Diba, F., Shimizu, M., & Hatano, R. (2011). Effects of soil aggregate size, moisture content and fertilizer management on nitrous oxide production in a volcanic ash soil. *Soil Science & Plant Nutrition*, *57*, 733–747. <https://doi.org/10.1080/00380768.2011.604767>
- Dong, W., Wang, Y., & Hu, C. (2013). Concentration profiles of CH₄, CO₂ and N₂O in soils of a wheat–maize rotation ecosystem in North China plain, measured weekly over a whole year. *Agriculture, Ecosystems and Environment*, *1*, 260–272. <https://doi.org/10.1016/j.agee.2012.10.004>
- Fujikawa, T., & Miyazaki, T. (2005). Effects of bulk density and soil type on the gas diffusion coefficient in repacked and undisturbed soils. *Soil Science*, *170*, 892–901. <https://doi.org/10.1097/01.ss.0000196771.53574.79>
- Giles, M. E., Daniell, T. J., & Baggs, E. M. (2017). Compound driven differences in N₂ and N₂O emission from soil; the role of substrate use efficiency and the microbial community. *Soil Biology and Biochemistry*, *106*, 90–98. <https://doi.org/10.1016/j.soilbio.2016.11.028>
- Goldberg, S. D., & Gebauer, G. (2009). Drought turns a Central European Norway spruce forest soil from an N₂O source to a transient N₂O sink. *Global Change Biology*, *15*, 850–860. <https://doi.org/10.1111/j.1365-2486.2008.01752.x>
- Goldberg, S. D., Knorr, K. H., & Gebauer, G. (2008). N₂O concentration and isotope signature along profiles provide deeper insight into the fate of N₂O in soils. *Isotopes in Environmental and Health Studies*, *44*, 377–391. <https://doi.org/10.1080/10256010802507433>
- Groffman, P. M., Altabet, M. A., Böhlke, H., Butterbach-Bahl, K., David, M. B., Firestone, M. K., Giblin, A. E., Kana, T. M., Nielsen, L. P., & Voytek, M. A. (2006). Methods for measuring

- denitrification: Diverse approaches to a difficult problem. *Ecological Applications*, 16, 2091–2122.
- Guo, L., & Lin, H. (2018). Addressing two bottlenecks to advance the understanding of preferential flow in soils, 1st ed. *Advances in Agronomy*, 147, 61–117. <https://doi.org/10.1016/bs.agron.2017.10.002>
- Harris, E., Diaz-Pines, E., Stoll, E., Schloter, M., Schulz, S., Duffner, C., Li, K., Moore, K. L., Ingrisch, J., Reinthaler, D., Zechmeister-Boltenstern, S., Glatzel, S., Brüggemann, N., & Bahn, M. (2021). Denitrifying pathways dominate nitrous oxide emissions from managed grassland during drought and rewetting. *Science Advances*, 7, eabb7118. <https://doi.org/10.1126/sciadv.abb7118>
- Hashimoto, S., & Komatsu, H. (2006). Relationships between soil CO₂ concentration and CO₂ production, temperature, water content, and gas diffusivity: Implications for field studies through sensitivity analyses. *Journal of Forest Research*, 11, 41–50. <https://doi.org/10.1007/s10310-005-0185-4>
- Hill, A. R., & Cardaci, M. (2004). Denitrification and organic carbon availability in riparian wetland soils and subsurface sediments. *Soil Science Society of America Journal*, 68, 320–325. <https://doi.org/10.2136/sssaj2004.3200a>
- Jahangir, M. M. R., Khalil, M. I., Johnston, P., Cardenas, L. M., Hatch, D. J., Butler, M., Barrett, M., O'flaherty, V., & Richards, K. G. (2012). Denitrification potential in subsoils: A mechanism to reduce nitrate leaching to groundwater. *Agriculture, Ecosystems & Environment*, 147, 13–23. <https://doi.org/10.1016/j.agee.2011.04.015>
- Jia, G., Shevliakova, E., Artaxo, P., Noblet-Ducoudré, D., Nathalie, H., Richard, Anderegg, W., Bernier, P., Carlo Espinoza, J., Semenov, S., Xu, X., Shevliakova, E., Artaxo, P., De Noblet-Ducoudré, N., Houghton, R., House, J., Kitajima, K., Lennard, C., Popp, A., Sirin, A., ... Verchot, L. (2019). Land-climate interactions. In P. R. Shukla, J. Skea, E. C. Buendia, V. Masson-Delmotte, H.-O. Pörtner, D. C. Roberts, P. Zhai, R. Slade, S. Connors, R. van Diemen, M. Ferrat, E. Haughey, S. Luz, S. Neogi, M. Pathak, J. Petzold, J. P. Pereira, P. Vyas, E. Huntley, et al. (Eds.), *Climate change and land: An IPCC special report on climate change, desertification, land degradation, sustainable land management, food security, and greenhouse gas fluxes in terrestrial ecosystems* (pp. 131–248).
- Khalil, M. I., Rosenani, A. B., Van Cleemput, O., Fauziah, C. I., & Shamsuddin, J. (2002). Nitrous oxide emissions from an ultisol of the humid tropics under maize-groundnut rotation. *Journal of Environmental Quality*, 31, 1071–1078. <https://doi.org/10.2134/jeq2002.1071>
- Laughlin, R. J., & Stevens, R. J. (2002). Evidence for fungal dominance of denitrification and codenitrification in a grassland soil. *Soil Science Society of America Journal*, 66, 1540–1548. <https://doi.org/10.2136/sssaj2002.1540>
- Laughlin, R. J., Stevens, R. J., & Zhuo, S. (1997). Determining nitrogen-15 in ammonium by producing nitrous oxide. *Soil Science Society of America Journal*, 61, 462. <https://doi.org/10.2136/sssaj1997.03615995006100020013x>
- Law, C. S., Watson, A. J., & Liddicoat, M. I. (1994). Automated vacuum analysis of sulphur hexafluoride in seawater: Derivation of the atmospheric trend (1970–1993) and potential as a transient tracer. *Marine Chemistry*, 48, 57–69. [https://doi.org/10.1016/0304-4203\(94\)90062-0](https://doi.org/10.1016/0304-4203(94)90062-0)
- Liu, R., Hu, H., Suter, H., Hayden, H. L., He, J., Mele, P., & Chen, D. (2016). Nitrification is a primary driver of nitrous oxide production in laboratory microcosms from different land-use soils. *Frontiers in Microbiology*, 7, 1373. <https://doi.org/10.3389/fmicb.2016.01373>
- Luo, J., Beule, L., Shao, G., Veldkamp, E., & Corre, M. D. (2022). Reduced soil gross N₂O emission driven by substrates rather than denitrification gene abundance in cropland agroforestry and monoculture. *Journal of Geophysical Research: Biogeosciences*, 127, 1–16. <https://doi.org/10.1029/2021jg006629>
- Miranda, K. M., Espey, M. G., & Wink, D. A. (2001). A rapid, simple spectrophotometric method for simultaneous detection of nitrate and nitrite. *Nitric Oxide*, 5(1), 62–71. <https://doi.org/10.1006/niox.2000.0319>
- Mulvaney, R. L. (1996). Nitrogen inorganic forms. In: D. L. Sparks, A. L. Page, P. A. Helmke, R. H. Loeppert (Eds.), *Methods of Soil Analysis. Part 3. Chemical Methods, ASA and SSSA, Madison* (pp. 1123–1184). <https://doi.org/10.2136/sssabookser5.3.c38>
- Müller, C., Stevens, R. J., Laughlin, R. J., & Jäger, H. J. (2004). Microbial processes and the site of N₂O production in a temperate grassland soil. *Soil Biology and Biochemistry*, 36, 453–461. <https://doi.org/10.1016/j.soilbio.2003.08.027>
- Neftel, A., Flechard, C., Ammann, C., Conen, F., Emmenegger, L., & Zeyer, K. (2007). Experimental assessment of N₂O background fluxes in grassland systems. *Tellus B: Chemical and Physical Meteorology*, 59, 470–482. <https://doi.org/10.1111/j.1600-0889.2007.00273.x>
- Patureau, D., Bernet, N., & Moletta, R. (1996). Effect of oxygen on denitrification in continuous chemostat culture with *Comamonas* sp. SGLY2. *Journal of Industrial Microbiology & Biotechnology*, 16, 124–128. <https://doi.org/10.1007/bf01570072>
- Pihlatie, M., Syväsalo, E., Simojoki, A., Esala, M., & Regina, K. (2004). Contribution of nitrification and denitrification to N₂O production in peat, clay and loamy sand soils under different soil moisture conditions. *Nutrient Cycling in Agroecosystems*, 70, 135–141. <https://doi.org/10.1023/B:FRES.0000048475.81211.3c>
- R Core Team. (2017). *A language and environment for statistical computing*. R Foundation for Statistical Computing.
- Richardson, D., Felgate, H., Watmough, N., Thomson, A., & Baggs, E. (2009). Mitigating release of the potent greenhouse gas N₂O from the nitrogen cycle—Could enzymic regulation hold the key? *Trends in Biotechnology*, 27, 388–397. <https://doi.org/10.1016/j.tibtech.2009.03.009>
- Rocca, J. D., Hall, E. K., Lennon, J. T., Evans, S. E., Waldrop, M. P., Cotner, J. B., Nemergut, D. R., Graham, E. B., & Wallenstein, M. D. (2015). Relationships between protein-encoding gene abundance and corresponding process are commonly assumed yet rarely observed. *The ISME Journal*, 9, 1693–1699. <https://doi.org/10.1038/ismej.2014.252>
- Roco, C. A., Bergaust, L. L., Shapleigh, J. P., & Yavitt, J. B. (2016). Reduction of nitrate to nitrite by microbes under oxic conditions. *Soil Biology and Biochemistry*, 100, 1–8. <https://doi.org/10.1016/j.soilbio.2016.05.008>
- Rolston, D. E., & Moldrup, P. (2002). 4.3 Gas diffusivity. In J. H. Dane & C. G. Topp (Eds.), *Methods of soil analysis: Part 4 physical methods* (pp. 1113–1139). Wiley.
- Rosenkranz, P., Brüggemann, N., Papen, H., Xu, Z., Seufert, G., & Butterbach-Bahl, K. (2006). N₂O, NO and CH₄ exchange, and

- microbial N turnover over a Mediterranean pine forest soil. *Environmental Research*, 3, 121–133.
- Rudolph, J., Rothfuss, F., & Conrad, R. (1996). Flux between soil and atmosphere, vertical concentration profiles in soil, and turnover of nitric oxide: 1. Measurements on a model soil core. *Journal of Atmospheric Chemistry*, 23, 253–273. <https://doi.org/10.1007/BF00055156>
- Schlesinger, W. H. (2013). An estimate of the global sink for nitrous oxide in soils. *Global Change Biology*, 19, 2929–2931. <https://doi.org/10.1111/gcb.12239>
- Schlüter, S., Henjes, S., Zawallich, J., Bergaust, L., Horn, M., Ippisch, O., Vogel, H. J., & Dörsch, P. (2018). Denitrification in soil aggregate analogues—effect of aggregate size and oxygen diffusion. *Frontiers in Environmental Science*, 6, 1–10. <https://doi.org/10.3389/fenvs.2018.00017>
- Semedo, M., Wittorf, L., Hallin, S., & Song, B. (2020). Differential expression of clade I and II N₂O reductase genes in denitrifying *Thauera linaloolentis* 47Lol^T under different nitrogen conditions. *FEMS Microbiology Letters*, 367, 1–6. <https://doi.org/10.1093/femsle/fnaa205>
- Sextstone, A. J., Revsbech, N. P., Parkin, T. B., & Tiedje, J. M. (1985). Direct measurement of oxygen profiles and denitrification rates in soil aggregates. *Soil Science Society of America Journal*, 49, 645–651. <https://doi.org/10.2136/sssaj1985.03615995004900030024x>
- Shcherbak, I., & Robertson, G. P. (2019). Nitrous oxide (N₂O) emissions from subsurface soils of agricultural ecosystems. *Ecosystems*, 22, 1650–1663. <https://doi.org/10.1007/s10021-019-00363-z>
- Smith, M. S., & Tiedje, J. M. (1979). Phases of denitrification following oxygen depletion in soil. *Soil Biology and Biochemistry*, 11, 261–267. [https://doi.org/10.1016/0038-0717\(79\)90071-3](https://doi.org/10.1016/0038-0717(79)90071-3)
- Stuchiner, E. R., & von Fischer, J. C. (2022a). Using isotope pool dilution to understand how organic carbon additions affect N₂O consumption in diverse soils. *Global Change Biology*, 2, 4163–4179. <https://doi.org/10.1111/gcb.16190>
- Stuchiner, E. R., & von Fischer, J. C. (2022b). Characterizing the importance of denitrification for N₂O production in soils using natural abundance and isotopic labeling techniques. *Journal of Geophysical Research – Biogeosciences*, 127, e2021JG006555. <https://doi.org/10.1029/2021JG006555>
- Van Beek, C. L., Hummelink, E. W. J., Velthof, G. L., & Oenema, O. (2004). Denitrification rates in relation to groundwater level in a peat soil under grassland. *Biology and Fertility of Soils*, 39, 329–336. <https://doi.org/10.1007/s00374-003-0685-3>
- van Bochove, E., Bertrand, N., & Caron, J. (1998). In situ estimation of the gaseous nitrous oxide diffusion coefficient in a Sandy loam soil. *Soil Science Society of America Journal*, 62, 1178–1184. <https://doi.org/10.2136/sssaj1998.03615995006200050004x>
- Van Cleemput, O. (1998). Subsoils: Chemo- and biological denitrification, N₂O and N₂ emissions. *Nutrient Cycling in Agroecosystems*, 52, 187–194. <https://doi.org/10.1023/a:1009728125678>
- Van Groenigen, J. W., Zwart, K. B., Harris, D., & Van Kessel, C. (2005). Vertical gradients of δ¹⁵N and δ¹⁸O in soil atmospheric N₂O—Temporal dynamics in a sandy soil. *Rapid Communications in Mass Spectrometry*, 19, 1289–1295. <https://doi.org/10.1002/rcm.1929>
- von Fischer, J. C., & Hedin, L. O. (2002). Separating methane production and consumption with a field-based isotope pool dilution technique. *Global Biogeochemical Cycles*, 16, 8–13. <https://doi.org/10.1029/2001gb001448>
- Wang, Y., Li, X., Dong, W., Wu, D., Hu, C., Zhang, Y., & Luo, Y. (2018). Depth-dependent greenhouse gas production and consumption in an upland cropping system in northern China. *Geoderma*, 319, 100–112. <https://doi.org/10.1016/j.geoderma.2018.01.001>
- Wen, Y., Chen, Z., Dannenmann, M., Carminati, A., Willibald, G., Kiese, R., Wolf, B., Veldkamp, E., Butterbach-Bahl, K., & Corre, M. D. (2016). Disentangling gross N₂O production and consumption in soil. *Scientific Reports*, 6, 1–8. <https://doi.org/10.1038/srep36517>
- Wen, Y., Corre, M. D., Schrell, W., & Veldkamp, E. (2017). Gross N₂O emission and gross N₂O uptake in soils under temperate spruce and beech forests. *Soil Biology and Biochemistry*, 112, 228–236. <https://doi.org/10.1016/j.soilbio.2017.05.011>
- Wickham, H. (2016). *Elegant Graphics for Data Analysis*. ggplot2.
- WRB. (2014). *World Reference Base (WRB) for soil resources (updated 2015). International soil classification system for naming soils and creating legends for soil maps*. World Soil Resources Reports No. 106. FAO.
- Wu, D., Dong, W., Oenema, O., Wang, Y., Trebs, I., & Hu, C. (2013). N₂O consumption by low-nitrogen soil and its regulation by water and oxygen. *Soil Biology and Biochemistry*, 60, 165–172. <https://doi.org/10.1016/j.soilbio.2013.01.028>
- Yang, W. H., & Silver, W. L. (2016). Net soil-atmosphere fluxes mask patterns in gross production and consumption of nitrous oxide and methane in a managed ecosystem. *Biogeosciences*, 13, 1705–1715. <https://doi.org/10.5194/bg-13-1705-2016>
- Yang, W. H., Teh, Y. A., & Silver, W. L. (2011). A test of a field-based ¹⁵N-nitrous oxide pool dilution technique to measure gross N₂O production in soil. *Global Change Biology*, 17, 3577–3588. <https://doi.org/10.1111/j.1365-2486.2011.02481.x>
- Zhang, Y., Mu, Y., Zhou, Y., Tian, D., Liu, J., & Zhang, C. (2016). NO and N₂O emissions from agricultural fields in the North China plain: Origination and mitigation. *Science of the Total Environment*, 551–552, 197–204. <https://doi.org/10.1016/j.scitotenv.2016.01.209>
- Zona, D., Janssens, I. A., Gioli, B., Jungkunst, H. F., Serrano, M. C., & Ceulemans, R. (2013). N₂O fluxes of a bio-energy poplar plantation during a two years rotation period. *GCB Bioenergy*, 5, 536–547. <https://doi.org/10.1111/gcbb.12019>

SUPPORTING INFORMATION

Additional supporting information can be found online in the Supporting Information section at the end of this article.

How to cite this article: Button, E. S., Marsden, K. A., Nightingale, P. D., Dixon, E. R., Chadwick, D. R., Jones, D. L., & Cárdenas, L. M. (2023). Separating N₂O production and consumption in intact agricultural soil cores at different moisture contents and depths. *European Journal of Soil Science*, 74(2), e13363. <https://doi.org/10.1111/ejss.13363>